21. A. B. Bagdasyaryan, "Exact solutions of problems concerning the action of an explosion in a brittle hard medium," Izv. Akad. Nauk ArmSSR, Ser. Mekh., 21, Nos. 5, 6 (1968).

EXPLOSION IN A GRANULAR POROUS MEDIUM WITH VARIABLE DILATANCY

E. E. Lovetskii, V. K. Sirotkin, and E. V. Sumin

UDC 622.235.5+539.374

Correct description of the flow of a granular medium is very important in considering an explosion in a granular or brittle rock. The most important feature of the flow of such a medium arises from repacking effects, which result not only in shear deformation but also in irreversible bulk strain. Usually, this bulk deformation is described within the framework of a dilatancy model [1]. The magnitude and sign of the dilatancy velocity are substantially dependent on the pressure and density [2-5]. It is assumed at present [6-9] that the dilatancy velocity is constant for such a medium. However, such an assumption does not allow one to incorporate the real dynamic behavior of the medium or to consider the effects of the initial state on the results of the explosion.

Here we process experimental data to derive an expression for the dilatancy velocity as a function of the pressure and density. This result is used in determining the expansion of a spherical gas cavity in an elastoplastic dilating medium. Particular attention is given to the final characteristics of the medium near the cavity. No allowance is made for the strength difference between the undisrupted and disrupted media, although this can be done if one assumes that the adhesion is small by comparison with the dry friction.

1. We consider spherically symmetrical motion in an elastoplastic porous dilating medium, which is compressed by a lithostatic pressure p_h. The source of the motion is a cavity of initial radius a_0 filled with adiabatically expanding explosion gases of initial pressure p_0 and adiabatic parameter γ.

The motion is described by the equation of continuity and the equation of motion:

$$\frac{\partial \rho}{\partial t} + u\frac{\partial \rho}{\partial r} + \rho\left(\frac{\partial u}{\partial r} + 2\frac{u}{r}\right) = 0; \tag{1.1}$$

$$\rho\left(\frac{\partial u}{\partial t} + u\frac{\partial u}{\partial r}\right) = -\frac{\partial p}{\partial r} + \frac{4}{3}\frac{\partial \tau}{\partial r} + \frac{4\tau}{r}, \tag{1.2}$$

where r is the distance from the explosion center, t is the time, u is the mass velocity, and ρ is the current density. The tangential stress τ and the pressure p are given by $\tau = (1/2)(\sigma_r - \sigma_\varphi)$, $p = -(1/3)(\sigma_r + 2\sigma_\varphi)$, where σ_r and σ_φ are the radial and azimuthal components of the stress tensor.

The stress variation in the elastic-strain zone is related to the velocity by Hooke's law:

$$\frac{d\tau}{dt} = G\left(\frac{\partial u}{\partial r} - \frac{u}{r}\right), \quad \frac{dp}{dt} = -K\left(\frac{\partial u}{\partial r} + 2\frac{u}{r}\right), \tag{1.3}$$

where $d/dt = \partial/\partial t + u\partial/\partial r$, G is the shear modulus, and K is the bulk compression coefficient.

Plastic strain will occur if the condition for plastic flow is met. We take this condition in the Mises–Huber–Schleicher form:

$$\frac{2}{\sqrt{3}}|\tau| = \alpha(\Lambda)p + Y, \tag{1.4}$$

where $\alpha(\Lambda)$ is the coefficient of friction, which is dependent on the dilatancy velocity Λ and Y is the adhesion. The $\alpha(\Lambda)$ dependence has been derived in [1] by processing data for various types of sands and takes the form

$$\alpha(\Lambda) = \frac{1}{2.11}(1.52 + 1.38\Lambda - \Lambda^2). \tag{1.5}$$

Moscow. Translated from Zhurnal Prikladnoi Mekhaniki i Tekhnicheskoi Fiziki, No. 2, pp. 149-155, March-April, 1981. Original article submitted January 10, 1980.

0021-8944/81/2202-0266$07.50

During the plastic flow, the density of the broken rock alters on account of the elastic strain and of particle repacking, which leads to the dilatancy effect. The following is [1] the equation describing the volume deformation of the medium with the dilatancy effect in the spherically symmetrical case:

$$\frac{\partial u}{\partial r}+2\frac{u}{r}+\frac{1}{K}\left(\frac{\partial p}{\partial t}+u\frac{\partial p}{\partial r}\right)=\frac{2}{\sqrt{3}}\Lambda(p,\rho)\left|\frac{\partial u}{\partial r}-\frac{u}{r}-\frac{1}{G}\frac{d\tau}{dt}\right|. \tag{1.6}$$

Experiments [2-4] indicate that Λ is dependent on the pressure and density; in particular, it can take positive or negative values, which correspond to loosening and consolidation of the rock.

Dilatancy has been examined [3] in experiments on octahedral shear for sands. Curves relating the volume change to the axial deformation have been drawn for various pressures. The sand is loosened at low pressures (as pointed out in [5], the loosening corresponds to the current porosity m being less than the critical porosity $m_*(p)$ at a given pressure). The dilatancy velocity decreases as the pressure rises, and the sand begins to consolidate at high pressures. The state with the critical porosity is characterized by plastic shear without change of volume. As the deformation proceeds, each of the curves tends to a certain constant value, which corresponds to the porosity tending to the critical value. The curve for $m_*(p)$ is closely approximated by

$$m_*(p)=0.46-0.02\left(\ln\frac{p}{p_1}\right)^{1.35},$$

where p_1 is chosen from considerations of convenience as 1 kgf/cm^2. This formula implies that the critical porosity decreases as the mean pressure in the specimen rises. The expression for $\Lambda(p,\rho)$ was chosen as a function of the ratio ρ_*/ρ, where $\rho_*(p)=\rho_M(1-m_*(p))$ is the critical density corresponding to the critical porosity $m_*(p)$ and defined by $\Lambda(\rho_*)\equiv 0$. Here ρ_M is the density of the mineral components. The very simple form of $\Lambda(p,\rho)$ corresponding to this property is defined by

$$\Lambda(p,\rho)=\Lambda_0\left(1-\frac{\rho_*(p)}{\rho}\right).$$

The coefficient Λ_0 is determined from experimental data [6], which give $\Lambda_0=0.5$.

2. The system (1.1)-(1.6) may be written in finite-difference form by analogy with [10] and then has second-order accuracy in time and coordinate. An artificial linear-quadratic viscosity is introduced in order to smooth out the hydrodynamic discontinuities. The accuracy of the calculation was checked from the law of conservation for the total system energy. The coordinate net was recalculated during the solution [10], which involved increasing the dimensions of the Lagrangian spatial cell.

Figures 1-6 show the numerical results. Figure 1 shows the pressure as a function of the reduced distance $rW^{-1/3}$ $\left(W=\frac{4}{3}\pi a_0^3\frac{p_0}{\gamma-1}\right.$ is the explosion energy) for the three instants $t_1=6t_0$, $t_2=9t_0$, and $t_3=27t_0$ (curves 1-3, respectively). Here $t_0=a_0/c_l$ (c_l is the longitudinal-wave speed and v_0 is the initial volume). The arrows indicate the start of the plastic flow behind the front. Figures 1 and 3 describe the behavior of a medium with the initial porosity $m_0=15\%$ $(1-m_0=1/\rho_M v_0)$. The numerical calculations were performed with an initial lithostatic pressure $p_h=0.2$ kbar, $K=0.52$ Mbar, $G=0.24$ Mbar, and $\gamma=1.4$.

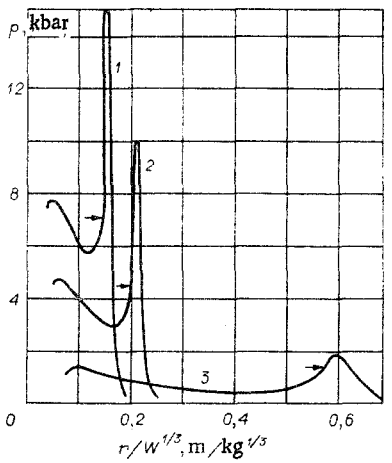

Fig. 1

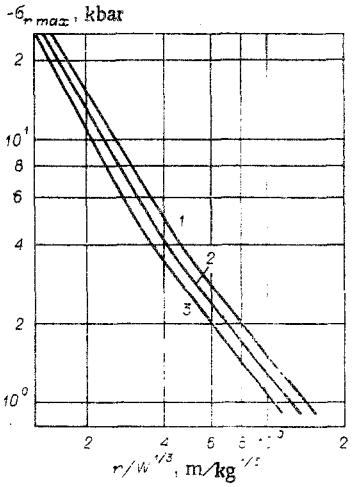

Fig. 2

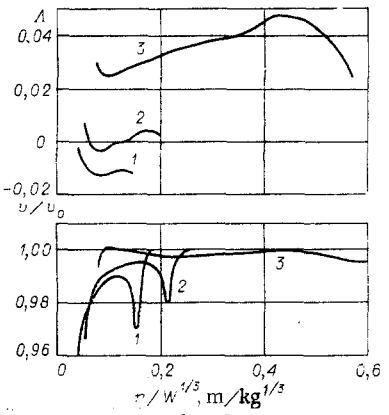

Fig. 3

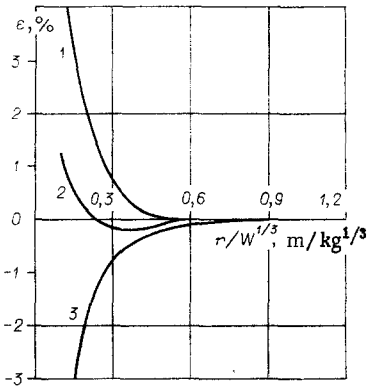

Fig. 4

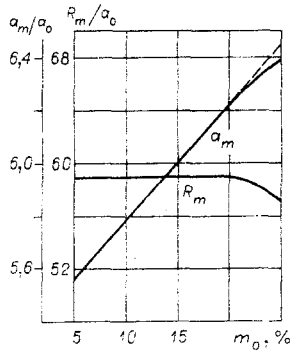

Fig. 5

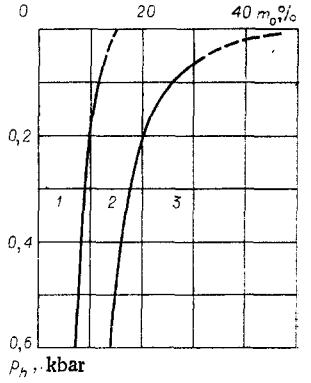

Fig. 6

Figure 1 shows that the distance dependence of the pressure is governed by two factors. Firstly, a compression wave propagates through the medium whose amplitude steadily decreases. Secondly, stresses arise near the cavity that are determined by the dynamics of the medium behind the compression-wave front. The distance dependence of these stresses is not monotonic. This behavior has been predicted from the solution to a model problem [8, 9]. This nonmonotonic behavior persists also in the residual stresses. The basic distance dependence of the residual stresses is analogous to that of [9].

The amplitude decay in the compression wave is substantially dependent on the initial porosity. Figure 2 shows the distance dependence of the maximal radial stresses $\sigma_{r\,max}$ in the compression wave for various porosities. Here curves 1-3 have been constructed for initial porosities of 5, 15, and 25%, respectively. There is a characteristic kink, whose coordinate r_* is described closely by

$$r_* W^{-1/3} = 0.56 - 0.9m.$$

This kink is due to detachment of the compression wave from the plastic-flow front and formation of an elastic precursor. The damping at small distances is of the form $\sigma_{r\,max} \sim r^{-\beta}$, where β is dependent on the porosity. For example, $\beta = 1.6$ for $m_0 = 5\%$, while $\beta = 1.8$ for $m_0 = 25\%$. Further, $\beta \approx 1$ for all porosities in the elastic region. The slight difference of β from one may be due to the use of the artificial viscosity.

We now consider the density change in the expansion of the cavity. The change is determined by the reversible elastic strains and the irreversible deformation associated with the dilatancy. Figure 3 shows graphs for the dilatancy velocity and relative specific volume v/v_0 in relation to reduced distance for the instants of Fig. 1 (curves 1-3, respectively). The volume change is basically elastic in the region of the compression wave, and the peak in the density is related to the elastic strain (minimum specific volume) in the region of the compression wave, as is evident from Fig. 3. Plastic flow begins directly behind the compression-wave front, and this results in irreversible bulk deformation associated with dilatancy. The α of (1.4) decreases as the initial porosity increases. Then the plastic-flow front approximates to the compression-wave front. If the porosity is sufficiently high ($m_0 > 40\%$), these two fronts coincide until the compression wave degenerates into the elastic precursor. The graph for Λ shows that there can be three states of irreversible deformation during the cavity expansion. In the initial stage, the pressure is high throughout the

region encompassed by the plastic flow, and the dilatancy velocity is negative, and therefore there is irreversible consolidation (curve 1 in Fig. 3). Then the dilatancy velocity becomes sign-varying (curve 2), but the shear strain is small at the initial stage of the explosive motion, so this has little effect on the curve for the specific volume. Subsequently, the pressure falls and the dilatancy velocity becomes positive throughout the plastic region (curve 3). The nonmonotonic dependence of the dilatancy velocity on the distance means that there is also a nonmonotonic behavior in the specific volume.

This picture in the dilatancy velocity is substantially dependent on the initial porosity. For example, only the first condition occurs for high porosities, where there is only consolidation. Also, the dilatancy coefficient is always positive for low initial porosities.

These features of the strain during the expansion are most prominent for the bulk residual strain ε ($\varepsilon = v/v_0 - 1$) as a function of distance, which is shown in Fig. 4. Curves 1-3 correspond to initial porosities of 5, 15, and 25%. At low porosities (curve 1), a loosening zone is formed near the cavity, whose size is approximately half the final radius of the plastic-flow zone. As the porosity increases (curve 2), the residual bulk strain shows a nonmonotone dependence on the reduced distance. Finally, curve 3 shows that there is a consolidation zone near the cavity. This behavior of the residual specific volume means that there is a zone of reduced porosity at reduced distances $rW^{-1/3} \simeq 0.25$-0.6. These results allow us to examine the behavior of the permeability k from the relationship between the latter and the porosity [11] $k \sim m^l$, where $l \simeq 10$ for sand. Therefore, here the nonmonotone behavior ε means that there is a zone of reduced permeability near the cavity.

Figure 5 shows the relative final radius of the cavity a_m/a_0 and the radius of the plastic-flow zone R_m/a_0 as functions of the initial porosity, which show that the final radius of the cavity increases linearly with the porosity. However, at $m_0 > 20\%$ the $a_m(m_0)$ dependence becomes nonlinear and a_m begins to increase more slowly. Also, R_m is constant at low porosities, while it begins to decrease slowly for $m_0 > 20\%$.

The final dimensions of the cavity and the plastic-flow zone are due to the following two factors. The loosening effect reduces the final radius of the cavity [7], while the final radius of the plastic-flow zone increases [9]. Also, the final values are substantially influenced by the coefficient of friction (strength of the medium). It has been shown [7, 9] that a_m and R_m decrease as the friction increases for $\Lambda = \text{const}$. The rise in porosity results in a fall in strength and a reduction in the dilatancy velocity. For low porosities, both factors favor increase in the final radius of the cavity. The dilatancy velocity becomes negative for $m_0 > 20\%$, and the $a_m(\Lambda)$ dependence becomes weaker in the region of negative Λ, while the $a_m(\alpha)$ dependence is unaltered. This means that the $a_m(m_0)$ dependence also becomes weaker. These factors balance out at small porosities as regards the final radius of the plastic-flow zone. The $R_m(\Lambda)$ dependence becomes stronger in the region of negative Λ, while the character of $R_m(\alpha)$ is unaltered. This results in the dependence of R_m on the initial porosity.

The variation in the porosity in the explosion is determined by m_0 and by p_h. We also examined the effects of lithostatic pressure on the bulk residual strain. Figure 6 shows the results for the following regions: residual loosening 1, residual consolidation 3, and nonmonotonic behavior of the residual porosity 2. The calculations were performed down to a lithostatic pressure p_h of 0.05 kbar, while for lower pressures they were extrapolated as indicated by the broken lines. Figure 6 also serves to define the permeability after the explosion. When the relation between the initial porosity and lithostatic pressure is as in region 1, there is an improvement in the filtration parameters in the plastic-flow zone. Region 2 corresponds to increased permeability near the cavity, but with a reduction in the permeability at large distances (Fig. 4). In region 3 there is a deterioration in the filtration parameters in the plastic-flow zone.

3. Here we have considered an explosion in a medium in which the dilatancy velocity and strength are dependent on the pressure and density. It has been found that the initial porosity has an appreciable effect on the propagation of the shock waves in a granular medium. In particular, the damping of the maximal radial stresses increases with the porosity, as does the final size of the cavity. The size of the plastic-flow zone is only slightly dependent on the initial porosity for $m_0 < 20\%$ and begins to decrease for $m_0 > 20\%$.

The initial porosity has its greatest effect on the behavior of the residual bulk strain. There is a change in the behavior of the residual strain from expansion to consolidation as the porosity and lithostatic pressure increase. At intermediate values of the porosity there may be nonmonotonic behavior of the bulk residual strain: expansion near the cavity and consolidation at larger distances.

We are indebted to A. N. Bovt and V. N. Nikolaevskii for useful discussions.

LITERATURE CITED

1. V. N. Nikolaevskii, N. M. Syrnikov, and G. M. Shefter, "Dynamics of elastoplastic dilating media," in: Advances in the Mechanics of Deformable Media [in Russian], Nauka, Moscow (1975).
2. A. W. Bishop, "The strength of soils as engineering materials," Geotechnique, 16, No. 2 (1966).
3. A. S. Vesic and G. W. Clough, "Behaviour of granular materials under high stresses," Proc. ASCE, J. Soil Mech. Found. Div., 94, No. 3 (1968).
4. S. L. Crouch, "Experimental determination of volumetric strain in failed rock," Int. J. Rock. Mech. and Mining Sci., 7, No. 6 (1970).
5. A. Cazagrande, "Character of cohesionless soils affecting the stability of slopes and earth fills," J. Boston Soc. Civil Eng., 257-276 (1936).
6. V. N. Rodionov, V. V. Alushkin, et al., The Mechanical Effect of an Underground Explosion [in Russian], Nedra, Moscow (1971).
7. S. Z. Dunin and V. K. Sirotkin, "Expansion of a gas cavity in a brittle rock on the basis of the dilatancy of the soil," Zh. Prikl. Mat. Tekh. Fiz., No. 4 (1977).
8. S. G. Artyshev and S. Z. Dunin, "Shock waves in dilating and nondilating media," Zh. Prikl. Mat. Tekh. Fiz., No. 4 (1978).
9. S. Z. Dunin, V. K. Sirotkin, and E. V. Sumin, "The state of the medium near a cavity expanding in a dilating medium," Zh. Prikl. Mat. Tekh. Fiz., No. 3 (1979).
10. M. L. Wilkins, "Calculation of elastoplastic flows," in: Computational Methods in Hydrodynamics [Russian translation], Mir, Moscow (1967).
11. V. N. Nikolaevskii, K. S. Basniev, et al., Mechanics of Saturated Porous Media [in Russian], Nedra, Moscow (1970).